DEVELOPMENT OF MARTIAN REGOLITH DURICRUST SIMULANTS FOR USE IN ROVER HAZARD DETECTION AND AVOIDANCE EXPERIMENTS. M. M. Battler[1, 2], M. Cross[1], M. Safdar[3], K. McIsaac[1], and M. Faragalli[4]. [1]Dept. of Electrical and Computer Engineering and Centre for Planetary Science and Exploration (CPSX), Western University, 1151 Richmond St., London ON, N6A 3K7, Canada. mbattle@uwo.ca, [2]Dept. of Earth Sciences, Western University, 1151 Richmond St., London ON, N6A 3K7, Canada, [3]Dept. of Civil and Environmental Engineering, Western University, 1151 Richmond St., London ON, N6A 3K7, Canada, [4]Mission Control Space Services, 1125 Colonel By Drive, 311 St. Patrick's Building Ottawa, ON K1S 5B6.

Introduction and Rationale: Most Mars surface missions to date have encountered duricrusts [1, 2, 3]. These surficial, weakly salt-cemented materials form due to the precipitation of minerals in the voids of soils. Duricrusts range from <1 cm to >10 cm in thickness, and have been fractured or penetrated by rover wheels or contact instruments. Regolith beneath a cemented crust can be very loose or weak, and therefore the collapse of a duricrust can cause rover mobility issues. Of particular relevance is the case of the indurated soil that was encountered by the rover Spirit. Spirit was immobilized when it broke through the crust and became embedded in unconsolidated fines [4, 5].

Current Mars rover driving strategies require human operators to study images of the terrain ahead of the rover to plan safe traverses. Research is now focusing on automating non-geometric hazard detection and terrain assessment via machine learning [6], though to date the efficiency and capability of operations workflows that incorporate these techniques have not been tested. Mission Control Space Services is developing an Autonomous Soil Assessment System (ASAS). ASAS combines proprioceptive and exteroceptive detection of soil properties to learn and facilitate the real-time identification of hazardous terrain ahead of Mars rovers, and minimize the necessity for human-in-the-loop decision-making. ASAS is currently at TRL 4 and being validated in several planetary analogue terrains.

The goals of this study were to: 1. Develop duricrust simulants with properties similar to those documented by previous Mars missions; 2. Characterize these materials with laboratory techniques to verify mineralogy and texture in order to validate the feasibility of non-contact detection; and 3. Enhance the current capabilities of ASAS to include autonomous detection and trafficability prediction of duricrusted terrain.

Background: Duricrust likely forms via the mobilization of salt ions within a layer of water adsorbed by regolith [1]. Recent modelling using humidity, temperature, and mineralogy data from Mars Science Laboratory (MSL) suggests there may be a daily water cycle on Mars, with transient brines forming nightly within the top 10's of cm's of the surface due to the absorption of atmospheric water vapour by hygroscopic salts, (e.g., perchlorates; [7]) and evaporation after sunrise. This is consistent with previous hypotheses [8, 9].

Results from the Viking Lander X-ray Fluorescence Spectrometer indicated that crusted soils contained significant concentrations of Cl and S [10]. Cementation by sulfate salts has been proposed to explain the higher sulfate abundance in duricrusts, with magnesium as the likely cation [11]. Numerous regions on Mars have intermediate thermal inertial and albedo values that are thought to be diagnostic of regionally extensive cemented material (duricrust) analogous to the smaller patches documented at landing sites [11]. The mechanism of formation of the crusts, the time scales involved, and the age of formation are still unconfirmed.

Duricrust Simulant Composition: Of the salts known to exist on Mars, sulfate salts are most abundant, followed by carbonates, chlorides, nitrates, and perchlorates [12]. In the literature, duricrusts have most commonly been associated with elevated S and Cl levels, however precise mineralogy measurements of martian duricrust have not been made. Therefore it is not clear which salts play the most important role in the formation of duricrusts. For the purpose of our study, we focused on sulfates and chlorides, due to their relative abundances on Mars, and the detections of S and Cl in associate with duricrust. Two of the most common types of sulfate minerals detected on Mars are calcium sulfates and magnesium sulfates. Conclusions from [9] and [11] indicate that magnesium sulfates are more likely to be involved with duricrust formation.

Therefore, in this study duricrust simulants were produced using varying concentrations of NaCl, Ca-sulfate, and Mg-sulfate, combined with Ottawa Sand, and "superfine grade" MMS-1 Mojave Mars Simulant, with particles smaller than 0.6mm.

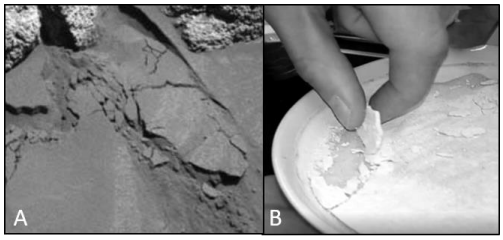

Fig. 1. A: 2-3 cm thick duricrust layer, Gusev Crater. Image 2P169853678EFFAAE0P2422L7M1. B: Duricrust simulant produced using Ottawa sand and sulfate salts; 3 mm thick.

Duricrust Simulant Production: Duricrust simulants were produced via three different methods of introducing and mixing the salt "ingredients" with MMS-1: air pluviation, 2. water pluviation, and 3. moist tamping. Dry air-pluviation closely replicates the particle fabric of aeolian sands, and water-pluviated samples replicate the particle fabric of fluvial and hydraulic fill sands [13, 14]. Moist tamping [15] replicates the particle fabric of moist-dumped fill sands [16]. In all cases, techniques used more water than is likely involved with duricrust formation on Mars. However, these techniques minimized compaction of the underlying loose sediment, therefore allowing for the production of a thin crust overlying unconsolidated fines.

Trials using different ratios and quantities of NaCl, Ca-sulfate, and Mg-sulfate were conducted first using a pure quartz sand (Ottawa Sand) until an optimal range of crust thicknesses and strengths was achieved. Next, the same ingredients and techniques were applied using MMS-1, and adjusted to account for minor sulfate and carbonate content native to the MMS-1. Samples were dried via oven heating at 120°C for 48 hrs to ensure the complete loss of moisture. To control for the role of heat in low temperature phase changes, additional samples were created and dried in low humidity/room temperature conditions, and in a vacuum chamber.

Duricrust Simulant Characterization: To verify composition, duricrust simulants were analyzed via Bruker D8 Discover Micro X-ray Diffractometer (XRD) at Western University's Powder and Micro XRD Facility. Additionally, samples were impregnated with epoxy and thin sections were made, to analyse cement texture and confirm cement mineralogy.

Additionally, duricrust simulants were analyzed using non-contact instruments similar to those that will be available on future Mars rovers, in order to identify distinguishing features that could be used by a trained classifier algorithm in the exterioceptive detection of duricrusts. These instruments included the PANalytical ASD TerraSpec Halo NIR spectrometer (on loan from NASA Ames), which provides reflectance spectral data in the 350-2500 nm range, and the Renishaw InVia Raman microscope at Western Surface Science. In particular, these instruments were used as proxies for components of the Mars 2020 SuperCam.

Results:

XRD: Duricrust production trials using MMS-1 proved to be challenging, as the MMS-1 source material contained a greater abundance of cementing agents than anticipated. XRD analysis of both dry and duricrusted samples indicated the (previously unreported) presence of clay minerals in MMS-1. This phenomenon of excessively cemented duricrust was observed in all cases where MMS-1 was used (oven-dried, room-temperature-dried, and vacuum-dried). Additional XRD analyses and thin section analyses are underway.

Spectroscopy: Based on the limited samples collected and the two instrument data sets, preliminary observations were made on classifying both the duricrust and non-crusted samples for machine learning purposes. Both instruments, and other similar field instruments, provide data in the form of spectral waveforms. The waveforms take on different shapes and characteristics dependent upon the sample and condition. For classification purposes, features need to be extracted from the waveforms. The following features were the most diagnostic from a machine-learning/ classification perspective: 1. For a given peak (or trough, in the case of absorption features), the: a. locations of peaks, b. prominences of peaks, and c. width of the peaks at half of the maximum value of the peak. 2. For NIR reflectance spectra, the average reflectance value. When the dry and duricrust samples were compared, the duricrust samples had a lower overall average reflectance.

Conclusions: This study has produced initial samples of simulated duricrusts, with chemical or physical similarities to true martian duricrust. A follow-on study will aim to produce chemically *and* physically accurate simulants, and will utilize additional non-contact characterization instruments to advance the capabilities of ASAS to detect and avoid duricrust.

Acknowledgements: This work was completed through a Natural Sciences and Engineering Research Council (NSERC) Engage grant to K. McIsaac. We thank R. Flemming for use of the microXRD, A. Sehlk and G. Osinski for use of the TerraSpec Halo, and T. Xie for assistance with the Raman microscope.

References: [1] Jakosky, B.M., & Christensen, P.R., (1986). J. Geophys. Res. 91, 3547-59. [2] Moore, H. et al., (1999). J. Geophys. Res. 104, 8729-46. [3] Arvidson, R.E., et al, (1989). Rev. Geophys. 27, 39-60. [4] Golombek, M. et al., (2006). J Geophys Res, 111, 2156-2202. [5] Arvidson, R.E., et al., (2010). J Geophys. Res, 115, E00F03. [6] Wong C. et al. (2017) IEEE Conf. AHS, 237-244. [7] Martín-Torres, F.J. et al., (2015), Nat. Geosci.8, 357-361. [8] Landis, G.A. et al., (2004), LPSC #2188. [9] Cabrol, N.A. et al. (2006). J. Geophys. Res. 111, E02S20. [10] Presley, M. A., and Christensen, P. R., (1989). LPSC #868. [11] Cooper, C.D., & Mustard, J. F. (2002). Icarus 158, 42-55. [12] Jones, E.G. (2017), IAC-17-F1.2.3. [13] Mulilis, J. P., et al. (1977). J. of Geotech. Eng. Div., ASCE 103, 91–108. [14] Vaid, Y. P, and Thomas, J, (1995). J. of Geotech. Eng., 121, 163-173. [15] Ladd, R.S. (1974). J. of Geotech. Eng. Div., ASCE 100, 1180-1184. [16] Safdar, M. et al., (2015). Int. J. Adv. Struc.Geotech. Eng., 4, 2319-5347.